

# Probing the superconducting gap symmetry of $\text{PrOs}_4\text{Sb}_{12}$ : A penetration depth study

Elbert E. M. Chia and M. B. Salamon

*Department of Physics, University of Illinois at Urbana-Champaign, 1110 W. Green St., Urbana IL 61801*

H. Sugawara and H. Sato

*Department of Physics, Tokyo Metropolitan University, Hachioji, Tokyo 192-0397, Japan*

(Dated: October 31, 2018)

We report measurements of the magnetic penetration depth  $\lambda$  in single crystals of  $\text{PrOs}_4\text{Sb}_{12}$  down to  $\sim 0.1$  K using a tunnel-diode based, self-inductive technique at 21 MHz, with the ac field applied along the  $a$ ,  $b$  and  $c$  directions. In all three field orientations the penetration depth and superfluid density  $\rho_s$  tend to follow a power law,  $\lambda \sim T^2$ ,  $\rho_s \sim T^2$  at low temperatures.  $\rho_s$  for various gap functions have been calculated, and data is best fit by the  $^3\text{He}$  A-phase-like gap with multidomains, each having two point nodes along a cube axis, and parameter  $\Delta_0(0)/k_B T_c = 2.6$ . This suggests that  $\text{PrOs}_4\text{Sb}_{12}$  is a strong-coupling superconductor with two point nodes on the Fermi surface. We also confirm the observation of the double transitions at 1.75 K and 1.85 K seen in other measurements.

The recent discovery of the Heavy Fermion (HF) skutterudite superconductor (SC)  $\text{PrOs}_4\text{Sb}_{12}$  [1, 2] has attracted much interest due to its differences with the other unconventional SC, and in particular, the HFSC.  $\text{PrOs}_4\text{Sb}_{12}$  has a nonmagnetic ground state of localized  $f$  electrons in the crystalline electric field, hence its HF behavior, and consequently the origin of its superconductivity, might be attributed to the interaction between the electric quadrupolar moments of  $\text{Pr}^{3+}$  and the conduction electrons. It is thus a candidate for the first SC mediated by quadrupolar fluctuations, i.e. by neither electron-phonon nor, as with other HFSC, magnetic interactions.

Recent experiments on  $\text{PrOs}_4\text{Sb}_{12}$  give conflicting evidence to the nature of the SC gap. Muon-spin rotation ( $\mu\text{SR}$ ) measurements revealed a low-temperature exponential behavior, suggesting isotropic pairing (either  $s$  or  $p$ -wave) [3]. Scanning tunneling spectroscopy measurements also measured a density of states (DOS) with no low-energy excitations with a well-developed SC gap over a large part of the Fermi Surface (FS) [4]. The absence of a Hebel-Slichter peak and the non- $T^3$  behavior of  $1/T_1$  in nuclear quadrupolar resonance (NQR) experiments suggest that  $\text{PrOs}_4\text{Sb}_{12}$  has a full gap or point nodes, but not line nodes, at zero field [5, 6]. If  $\text{PrOs}_4\text{Sb}_{12}$  has an isotropic gap, then it is unique among HFSC, suggesting the possibility of (a) an important difference in superconducting properties between HFSC with magnetic and non-magnetic  $f$ -ion ground states, and (b) a correlation between pairing symmetry (isotropic or nodal gap) and mechanism (quadrupolar or magnetic fluctuations) of superconductivity [3].

Unlike the  $\mu\text{SR}$  and NQR results, angle-dependent thermal conductivity measurements [7] revealed two distinct SC phases with different symmetries, a phase transition between them, and presence of *point* nodes. In the high-field phase four point nodes ([100] and [010] directions) have been observed, whereas there are only two

point nodes ([010] directions only) in the low-field phase. Specific-heat data [1] also show a low-temperature power law behavior, suggesting the presence of nodes. Another recent  $\mu\text{SR}$  experiment revealed the spontaneous appearance of static internal magnetic fields below  $T_c$ , providing evidence that the SC state is a time-reversal-symmetry-breaking (TRSB) state [8].

In this paper, we present high-precision measurements of penetration depths  $\lambda(T)$  of  $\text{PrOs}_4\text{Sb}_{12}$  at temperatures down to 0.1 K. The ac field was applied along all three crystallographic axes. In all three field orientations both  $\lambda(T)$  and superfluid density  $\rho_s(T)$  tends to follow a quadratic power law, suggesting that the SC gap has nodes on the FS.  $\rho_s$  for various gap functions has been calculated, and data are best fit by the  $^3\text{He}$  A-phase-like gap, with two point nodes in the [010] directions. Our data thus puts  $\text{PrOs}_4\text{Sb}_{12}$  in line with other HFSC, in that they all have nodes on the FS, despite the proposed non-magnetic nature of the mechanism of its superconductivity.

Details of sample growth and characterization are described in Ref. 9. Measurements were performed utilizing a 21-MHz tunnel diode oscillator [10] with a noise level of 2 parts in  $10^9$  and low drift. The magnitude of the ac field was estimated to be less than 5 mOe. The cryostat was surrounded by a bilayer Mumetal shield that reduced the dc field to less than 1 mOe. The sample was aligned inside the probing coil in all three crystallographic directions. The sample was mounted, using a small amount of GE varnish, on a single crystal sapphire rod. The other end of the rod was thermally connected to the mixing chamber of an Oxford Kelvinox 25 dilution refrigerator. The sample temperature is monitored using a calibrated  $\text{RuO}_2$  resistor at low temperatures ( $T_{\text{base}} - 1.8$  K), and a calibrated Cernox thermometer at higher temperatures (1.3 K - 2.5 K).

The deviation  $\Delta\lambda_i(T) = \lambda_i(T) - \lambda_i(0.1 \text{ K})$  ( $i = a, b, c$ ) is proportional to the change in resonant frequency

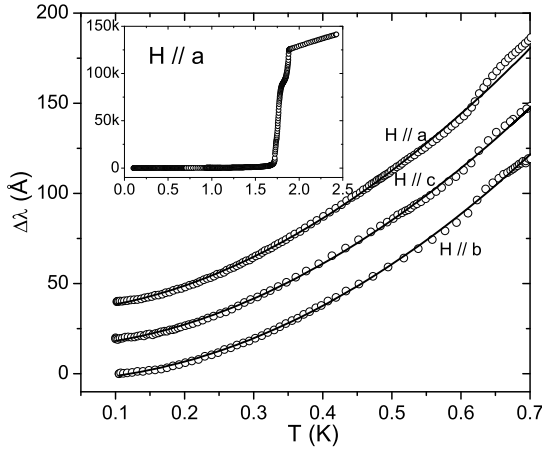


FIG. 1: Low-temperature dependence of the penetration depth  $\Delta\lambda(T)$  for field orientations  $H//a, b, c$ . The curves have been offset for clarity. The solid lines are fits to  $\Delta\lambda(T) = A + BT^n$  from 0.1 K to 0.55 K. Upper inset shows  $\Delta\lambda_a(T)$  over the full temperature range.

$\Delta f(T)$ , with the proportionality factor  $G$  dependent on sample and coil geometries. The subscript  $i$  denotes the direction of the applied magnetic field. For our  $H//a$  data, we determine  $G$  from a single-crystal sample of pure Al by fitting the Al data to extreme nonlocal expressions and then adjusting for relative sample dimensions [11]. Testing this approach on a single crystal of Pb, we found good agreement with conventional BCS expressions. The value of  $G_a$  obtained this way has an error of  $\pm 10\%$ , since our sample has a rectangular basal area instead of square [12]. To obtain  $G_b$  and  $G_c$  we make use of the cubic symmetry of the crystal and assume that the total change in penetration depth from the three orientations are equal, i.e.  $\Delta\lambda_a(T_c) = \Delta\lambda_b(T_c) = \Delta\lambda_c(T_c)$ . From this equality, and the value of  $G_a$ , we can calculate  $G_b$  and  $G_c$ .

Fig. 1 shows  $\Delta\lambda_i(T)$  as functions of temperature. All three curves vary strongly at low temperatures, inconsistent with exponential behavior expected for isotropic  $s$ -wave superconductors. On the other hand, the variation is not linear, but has an obvious upward curvature, unlike the low-temperature behavior expected for pure  $d$ -wave superconductors. A fit of the low temperature data (up to  $0.55\text{ K} \approx 0.3 T_c$ ) to a variable power law,  $\Delta\lambda(T) = A + BT^n$  yields  $n = 1.9 \pm 0.1$  for  $H//a, b$ , and  $n = 2.0 \pm 0.1$  for  $H//c$ . The uncertainty in  $n$  is *not* a consequence of the uncertainty in  $G$ , but rather of the somewhat uneven faces of the crystal and the range of fit. Within the uncertainty in  $G$  the three curves are consistent with one another. There is also a small upturn near 0.62 K, which might distort the low-temperature fit and cause the power law to deviate from  $T^2$ . The NQR spin-

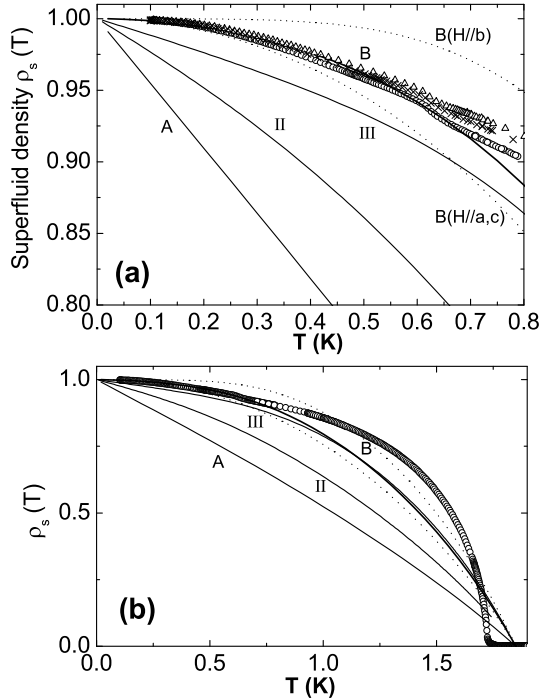


FIG. 2: (a) Low-temperature superfluid density  $\rho_s(T) = [\lambda^2(0)/\lambda^2(T)]$  calculated from  $\Delta\lambda(T)$  data in Fig. 1, for all three field orientations. (○)  $H//a$ , (△)  $H//b$ , (×)  $H//c$ . Using  $\Delta_0(0)/k_B T_c = 2.6$ , the solid lines are the calculated effective superfluid density  $\rho_s^{eff}$  corresponding to gaps II, III, A and B. The dotted lines correspond to  $\rho_s(H//b)$  and  $\rho_s(H//a, c)$  for gap B. (b) The same calculated curves over the entire temperature range. Only the  $\rho_s(T)$  data for  $H//a$  are shown.

lattice relaxation rate also changes around this temperature, however, the origin is not clear at present [5, 13]. A non-unitary state has the unique feature that spin-up and spin-down Cooper pairs have different excitation gaps [14]. If the SC state in  $\text{PrOs}_4\text{Sb}_{12}$  is a TRSB state, then this upturn may be due to the contribution from the smaller gap [8]. It is interesting to note that a fit of the  $\Delta\lambda(T)$  from 0.6 K to 1.1 K, to the same variable power law, gives an exponent of about 3, consistent with  $n \approx 4$  obtained for specific-heat data over the same temperature range [1].

Using the value of  $\lambda(0) = 3440\text{ \AA}$  from  $\mu\text{SR}$  measurements [3], we calculated the superfluid density  $\rho_s$  from our data. We follow the procedure in Ref. 11 to compute the experimental superfluid density, using the  $T^2$  fit to estimate the small difference between  $\lambda(0)$  and  $\lambda(0.1\text{ K})$ . Fig. 2a shows  $\rho_s(T)$  for all three field orientations at low temperatures. In each case, a fit of  $\rho_s(T)$  to a variable power law,  $\rho_s(T) = 1 - \alpha T^n$  also yields  $n \approx 2$ , from 0.1 K ( $\sim 0.05 T_c$ ) to 0.55 K. Once again this suggests the presence of low-lying excitations, incompatible with

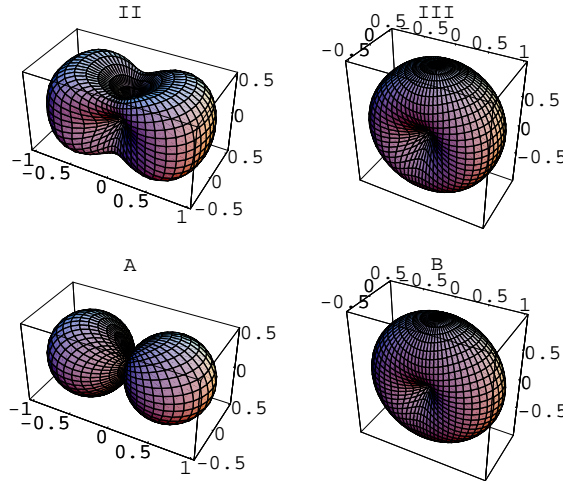


FIG. 3: Polar plots of gap functions (II), (III), (A) and (B).

an isotropic SC gap.

Several theoretical proposals have been put forward to understand the two SC phases [6, 15, 16]. To explain the behavior of the angle-dependent, magneto-thermal-conductivity results [7], Maki *et al.* [15] proposed three possible SC gap functions for  $\text{PrOs}_4\text{Sb}_{12}$ . In particular, for the low-field (L) phase, two gap functions were proposed: (II)  $f(\mathbf{k})=1 - k_y^4 - k_z^4$  having four nodes and (III)  $f(\mathbf{k})=1 - k_y^4$ , with two point nodes. The gap function is  $\Delta(\mathbf{k}) \equiv \Delta_0 f(\mathbf{k})$ , with the form factor  $f(\mathbf{k})$  normalized to unity and  $\Delta_0$  the temperature-*dependent* maximum gap value. As we will see, both functions lead to a linear temperature dependence for the superfluid density. Consequently, we consider two further gap functions: (A)  $\mathbf{d}(\mathbf{k})=\hat{y} k_a$  (a line-node gap), and (B)  $\mathbf{d}(\mathbf{k})=\hat{y} (k_a \pm ik_c)$ , for which  $\Delta(\mathbf{k})=\Delta_0 |\mathbf{d}(\mathbf{k})|$ . Gap B has two point nodes along the [010] directions and a gap dispersion identical to the superfluid  $^3\text{He}$  A-phase,  $\Delta(\mathbf{k})=\Delta_0 |k_a \pm ik_b|=\Delta_0 \sin \theta$ ; hence, they give identical temperature dependences of  $\rho_s$ . Polar plots of these gap functions are shown in Fig. 3. We have assumed the gap maximum  $\Delta_0(T)$  to have the form  $\Delta_0(T) = \delta_{sc} k T_c \tanh\{\frac{\pi}{\delta_{sc}} \sqrt{a(\frac{\Delta C}{C})(\frac{T_c}{T} - 1)}\}$  [17], where  $\delta_{sc} \equiv \Delta_0(0)/k_B T_c$  is the only variable parameter,  $T_c = 1.85$  K,  $a = 2/3$ , and the specific heat jump  $\Delta C/C = 3$  is an experimentally obtained value [18].

A problem arises immediately with point nodes. If there are only two point nodes in the [010] directions, breaking cubic symmetry, then one would expect  $\Delta \lambda_b$  to tend toward an exponential temperature dependence at low temperatures. We show this in Fig. 2, where we have calculated the superfluid density for gap B for fields along [010] and either [100] or [001]. A measurement along [010] would indeed give exponential behavior while measurements in orthogonal directions give a strong temperature dependence. However, our experimental data show

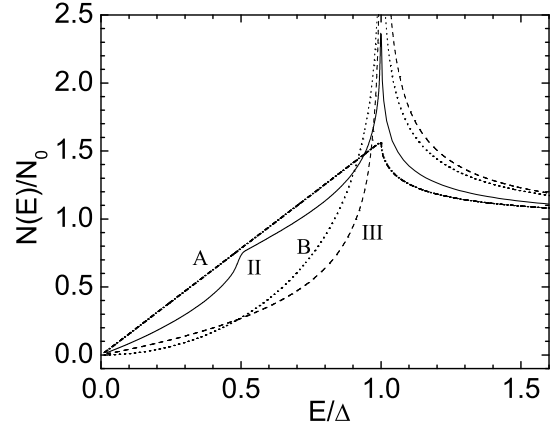


FIG. 4: Quasiparticle DOS for the gap functions II (full line), III (short-dashed line), A (short-dash-dotted line) and B (short-dotted line).

otherwise - there is an almost identical  $T^2$  superfluid response in all three field orientations. While it is possible that, in the absence of an external agent, the sample will randomly choose one, *and only one*, axis along which to locate the nodes each time it becomes superconducting, it is much more likely to develop a domain structure. One possibility is that the SC order parameter and strain are coupled [16], a situation similar to magnetostriction in ferromagnets. Such a situation also arises in Chromium (Cr) [19], where the coupling between the spin-density-wave (SDW) and strain wave causes the wave vector  $\mathbf{Q}$  of the modulation to point along any {001} direction in the bcc Cr lattice. In bulk Cr all three possible orientations occur with equal probability. A Cr single crystal thus has multiple domains, with each domain corresponding to one of three possible  $\mathbf{Q}_x$ ,  $\mathbf{Q}_y$  and  $\mathbf{Q}_z$  regions [20] - the “poly- $\mathbf{Q}$ ” state. Tensile stress is applied along one cube axis while cooling through  $T_N$ , however, produces a “single- $\mathbf{Q}$ ” state with all domains having their  $\mathbf{Q}$ ’s pointing in the same direction, along the stress axis [21]. Evidence that a domain with only two point nodes can form in  $\text{PrOs}_4\text{Sb}_{12}$  was reported in Ref. 7, where nodes were seen only along a single [010] axis. We suggest that the experimental setup of Ref. 7 may have strained the sample to produce a single domain, analogous to the single- $\mathbf{Q}$  state of Cr.

Assuming the existence of domains, we plot an effective superfluid density  $\rho_s^{eff}$  by taking the average of [100], [010] and [001]-superfluid densities, with equal weight from each component. The superfluid densities in different directions are evaluated using the expression

$$\rho_s(H/x) = 1 - \frac{3}{N(0)} \sum_{\mathbf{k}} (\hat{k}_y^2 + \hat{k}_z^2) \frac{\partial f}{\partial E_{\mathbf{k}}} \quad (1)$$

where  $x, y, z = \text{any permutation of } a, b, c$ .  $N(0)$  is the quasiparticle DOS at the FS,  $f = [\exp(E_{\mathbf{k}}/k_B T) + 1]^{-1}$  is the Fermi function, and  $E_{\mathbf{k}} = [\varepsilon^2(\mathbf{k}) + \Delta(\mathbf{k}, T)^2]^{1/2}$  is the quasiparticle energy. The component superfluid densities for Gap B are shown as two dotted lines, and  $\rho_s^{eff}$  as a solid line, in Fig. 2. Clearly, the agreement between data and  $\rho_s^{eff}$  is very good. We chose the strong-coupling value  $\delta_{sc} = 2.6$  here, taken from Ref. 5. Using  $\delta_{sc} = 2.1$  from Ref. 3 gives a worse fit. For the other gap functions, we also calculated  $\rho_s^{eff}$  (shown in Fig. 2) and  $\rho_s(H//a, b, c)$  (not shown here) - all of them give linear temperature dependences and fall far from the experimental data. The effective quasiparticle DOS for all four gap functions are also shown in Fig. 4. Our data therefore suggest that  $\text{PrOs}_4\text{Sb}_{12}$  is a strong-coupling unconventional SC. The superfluid data is best fit with a  $^3\text{He}$  A-phase-like gap, with two point nodes on its FS. Both the field-direction-independence of the superfluid data, and the nice fit of the data to  $\rho_s^{eff}$ , strongly suggest that  $\text{PrOs}_4\text{Sb}_{12}$  has multidomains. Note that though Gap B is a unitary gap, our low- $T$  data can also be fit [22] by the two-point-node L-phase *non-unitary* gap proposed by Ichioka *et al.* in Ref. 6, with similar DOS structure. Hence our data does not contradict the non-unitary result of Aoki *et al.* [8].

It is already apparent in Fig. 2a that the data deviate from the proposed gap function above 0.6 K. This is even clearer in Fig. 2b, which shows  $\rho_s(T)$  for  $H//a$  from 0.1 K to  $T_c$ . The other two field orientations give almost identical temperature dependence. None of the four gap functions fits the data over this larger temperature range. This could be due to the opening up of the smaller gap caused by the non-unitarity of the SC state, as mentioned earlier. Also, strong changes in the mass renormalization in different sheets have been found in de Haas van Alphen experiments [9]. These changes may cause the distribution of values of the SC gap measured in tunneling measurements [4], and strengthens both the idea that the mass renormalization and superconductivity are of the same origin, i.e. that the quadrupolar fluctuations favor SC correlations, as well as the possible multiband character of superconductivity in this material [4]. Hence a multiband analysis, similar to those performed on  $\text{MgB}_2$ , might be required to fit the superfluid data over the entire temperature range.

Finally, we turn to the region near  $T_c$ . Fig. 5 shows  $\Delta\lambda(T)$  near  $T_c$  for all three field orientations. Three features can be seen: the onset of superconductivity at 1.88 K, a strong but broad shoulder near 1.8 K, and finally a weak shoulder near 1.74 K (observable even in the  $H//c$  data). In another sample from the same batch, only the first and third features were observed. The 1.88 K and 1.74 K features confirm the two superconducting transitions seen in the specific-heat measurement [18], and suggested by angle-dependent thermal conductivity measurements [7]. The origin of the 1.8 K shoulder is

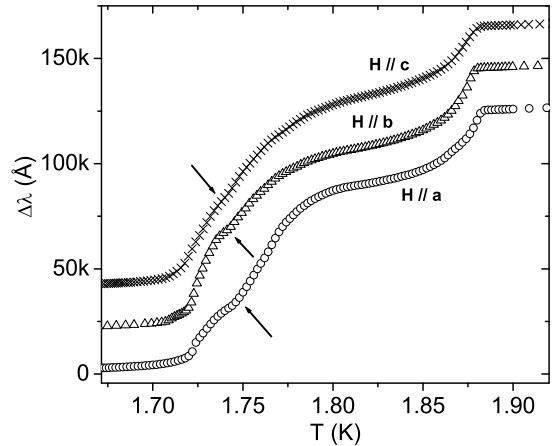


FIG. 5:  $\Delta\lambda(T)$  for all three field orientations near  $T_c$ . The curves have been offset for clarity. The arrows indicate the second superconducting transition at 1.74 K.

unknown. In the  $\rho_s(T)$  plot,  $\rho_s$  already approaches zero near 1.7 K. So these features were not discernible there. Also, we did not see any anomaly around  $T^* = 2.3$  K that was observed in Ref. 5.

In conclusion, we report measurements of the magnetic penetration depth  $\lambda$  in single crystals of  $\text{PrOs}_4\text{Sb}_{12}$  down to 0.1 K using a tunnel-diode based, self-inductive technique at 21 MHz, with the ac field applied along the  $a$ ,  $b$  and  $c$  directions. In all three field orientations  $\lambda$  and superfluid density  $\rho_s$  tend to follow a quadratic power law. We have calculated  $\rho_s$  for various gap functions, finding that the data are best fit by the  $^3\text{He}$  A-phase-like gap function with two point nodes on the FS. We also observe the double transitions near 1.75 K and 1.85 K seen in other measurements.

One of the authors (E.E.M.C.) acknowledges D. Lawrie and Y. Matsuda for useful discussions. Special thanks to K. Machida for significant contributions. This work was supported by the NSF through Grant No. DMR99-72087.

---

- [1] E. D. Bauer *et al.*, Phys. Rev. B **65**, 100506 (R) (2002).
- [2] M. B. Maple *et al.*, J. Phys. Soc. Jpn., Suppl. B **71**, 23 (2002).
- [3] D. E. MacLaughlin *et al.*, Phys. Rev. Lett. **89**, 157001 (2002).
- [4] H. Suderow *et al.*, cond-mat/0306463 (2003).
- [5] H. Kotegawa *et al.*, Phys. Rev. Lett. **90**, 027001 (2003).
- [6] M. Ichioka, N. Nakai, and K. Machida, J. Phys. Soc. Jpn. **72**, 1322 (2003).
- [7] K. Izawa *et al.*, Phys. Rev. Lett. **90**, 117001 (2003).
- [8] Y. Aoki *et al.*, Phys. Rev. Lett. **91**, 067003 (2003).
- [9] H. Sugawara *et al.*, Phys. Rev. B **66**, 220504 (R) (2002).

- [10] I. Bonalde *et al.*, Phys. Rev. Lett. **85**, 4775 (2000).
- [11] E. E. M. Chia *et al.*, Phys. Rev. B **67**, 014527 (2003).
- [12] R. Prozorov, R. W. Gianetta, A. Carrington, and F. M. Araujo-Moreira, Phys. Rev. B **62**, 115 (2000).
- [13] H. Sugawara, private conversation .
- [14] M. Sigrist and K. Ueda, Rev. Mod. Phys. **63**, 239 (1991).
- [15] K. Maki *et al.*, cond-mat/0212090 (2002).
- [16] J. Goryo, Phys. Rev. B **67**, 184511 (2003).
- [17] F. Gross *et al.*, Z. Phys. B **64**, 175 (1986).
- [18] R. Vollmer *et al.*, Phys. Rev. Lett. **90**, 057001 (2003).
- [19] E. Fawcett, Rev. Mod. Phys. **60**, 209 (1988).
- [20] S. A. Werner, A. Arrott, and H. Kendrick, J. Appl. Phys. **37**, 1260 (1966).
- [21] T. J. Bastow and R. Street, Phys. Rev. **141**, 51 (1966).
- [22] K. Machida, private conversation .